

Tunneling and percolation in metal-insulator composite materials

D. Toker, D. Azulay, N. Shimoni, I. Balberg, and O. Millo*

The Racah Institute of Physics, The Hebrew University, Jerusalem 91904, Israel

(Received 24 April 2003; published 25 July 2003)

In many composites, the electrical transport takes place only by tunneling between isolated particles. For a long time, it was quite a puzzle how, in spite of the incompatibility of tunneling and percolation networks, these composites conform well to percolation theory. We found, by conductance atomic force microscopy measurements on granular metals, that it is the apparent cut off of the tunneling to non-nearest-neighbors that brings about this behavior. In particular, the percolation cluster is shown to consist of the nearest-neighbors subnetwork of the full tunneling network.

DOI: 10.1103/PhysRevB.68.041403

PACS number(s): 68.37.Ps, 72.80.Tm, 61.43.Hv, 81.05.Rm

The electrical conduction in composite systems comprising an intricate network of conducting and insulating phases is determined by two mechanisms, percolation in a continuous conducting network¹ and/or tunneling^{2,3} between isolated conducting particles (grains, crystallites, etc.). In the pioneering works on such systems, these two mechanisms have been considered separately.^{1,2,3,4,5,6} In particular, for a high enough content of the metallic phase in granular metals, a continuous network is formed by the coalescence of the metallic grains. This continuity yields, as expected from “classical” percolation theory,⁷ the typical power-law dependence of the electrical conductivity σ on the vol % of the conducting phase x :

$$\sigma \propto (x - x_c)^t, \quad (1)$$

where t is a corresponding critical exponent. The value of x_c that was derived by fitting^{1,5} Eq. (1) to the experimental data on granular metals is in excellent agreement with that extracted from structural and other physical data,^{4,5} which shows the formation of a continuous metallic network. Moreover, the conductivity exponent was found to be very close to the predicted⁷ universal value of $t=2.0$, confirming that the value derived experimentally for x_c is exactly the (global geometrical connectivity) threshold that is considered in percolation theory.^{7,8} On the other hand, in contrast with the expectation from percolation theory,⁷ a considerable finite conductivity was observed in the regime of $x < x_c$ (the so-called dielectric regime^{4,5}), where a continuous metallic network is absent. This conductivity was attributed to interparticle tunneling.^{2,4,9,10} However, while the theories proposed to account for the electrical conductance in this regime have considered the tunneling within a single pair of adjacent particles, the global electrical connectedness of the tunneling conduction network has not been discussed. This approach was also carried over to other composites,^{3,6} where the particles do not coalesce or fuse¹¹ for any x .

While *a priori* justified, the latter approach has been ignored by numerous authors, and transport in systems lacking a continuous geometrical network of the conducting phase, such as carbon black-polymer^{12,13,14} and other^{15,16} composites, was analyzed in terms of percolation theory. Surprisingly, an excellent agreement was found^{12,13,14,15,16} between corresponding experimental results and the predictions of

percolation theory. In particular, agreement was found, by applying Eq. (1), with universal¹² or nonuniversal^{17,18} values of t . However, the meaning and the values of x_c , which were found from these fits, were not discussed, and the applicability of the above phenomenological percolation approach has not yet been justified.

When attempting to find such a justification and the meaning of x_c , one immediately notes that a system of separated conducting particles with tunneling conduction is *a priori* incompatible¹⁹ with the percolation picture. Geometrically, no two particles are in contact (and then no well-defined percolation cluster and percolation threshold are apparent), and electrically all particles are in contact with each other by tunneling (and then no percolation transition in the electrical properties is expected). In the composites considered, we have a homogeneous network of tunneling conductors, to which we refer here as all-connected tunneling network (ACTN). The question that arises then is how is it that, in spite of this global tunneling connectivity of the network, the electrical conduction in corresponding composites is governed by the very well-defined percolationlike behavior.^{14,19} The purpose of the present paper is to resolve this issue, thus providing an *a posteriori* justification for applying^{12,13,14,15,16,17,18} the percolation approach to the analysis of noncontinuous conducting networks. In particular, we will show that x_c has a well-defined meaning in such systems, and argue that the ACTN can be reduced to a well-defined percolation network, such as in porous media²⁰ where the geometrical and electrical networks coincide. To this end, one would like to obtain local current maps of these systems, or a geometrical-statistical property that can account for them, such as the fractal dimension of the current-carrying percolation cluster.

Following the success of the application of conductance atomic force microscopy (C-AFM) to granular metals²¹ and our ability²² to derive experimentally (with high accuracy) that fractal dimension of the percolation cluster in carbon black-polymer composites (CBPC), we have applied this method to the present study of granular metals. The basic idea of this work on Ni-SiO₂ composites is then to discriminate between various current maps by their fractal dimension. As we show below, this approach is found useful for providing an answer to the above questions, for granular

metals in the $x < x_c$ regime in particular, and for two-phase composites where the conducting particles are geometrically separated in general.

The Ni-SiO₂ films, 2.5–5.5 μm thick and 5 mm wide, were deposited as we described previously²³ on Pyrex substrates by cosputtering of Ni and SiO₂. The cosputtering method^{4,5} enables a continuous variation of the metal content (vol % Ni) along the deposited film, where one end is Ni rich and the other end is insulator rich. The typical size of the Ni particles increases continuously from 4 nm at $x = 35$ vol % to 10 nm at $x = 50$ vol %, to a continuous network at $x = 90$ vol %.^{4,5,23,24} For the electrical measurements, Cu-Au electrodes were predeposited on the substrate, with a separation of 2.54 mm. The resistance along the substrate sections was determined by a standard four-probe technique. For the C-AFM measurements, some of the samples were cut out, leaving on each sample an electrode that served as a counterelectrode to the scanning conducting AFM tip. For these measurements, we have used samples with Ni contents of 24, 28, 35, 47, 60, 72, 80, 87, and 92 vol %. The details of our C-AFM apparatus and the procedure of our measurements were presented recently²² and will not be repeated here. We point out, however, that the spatial resolution of the current images was limited only by the pixel size (typically $10 \times 10 \text{ nm}^2$) and that, since the tip was scanning more than 1 mm from the counterelectrode, the measured current images reflect two-dimensional cross sections of the three-dimensional macroscopic conduction network. We refer to areas of the image where current from the tip to the counterelectrode is detected as “conducting islands,” and the lowest current that we consider in the analysis of an image is denoted as the “cutoff current” I_{co} .²² Obviously, the total area covered by the conducting islands, A_t , depends on the chosen I_{co} . The larger the considered I_{co} , the smaller the A_t , since only lower resistance paths of the conduction network are included. We point out that no correlation was found between the AFM topographic images and the C-AFM images, implying that the current maps reflect mainly the electrical properties of the bulk of the sample.²²

To characterize our samples, we show in Fig. 1 the dependence of the conductivity on the Ni vol %. These results are much the same as those obtained on many granular metals.^{1,4,5,25} For x values beyond a certain critical value x_c , the electrical conductivity follows the expected universal percolation behavior with $t \approx 2$, as shown by the corresponding fit to Eq. (1). The value of $x_c = 52$ vol % found here is in excellent agreement with previous electrical and structural measurements performed on this system.^{5,23,24,25} The non-negligible “excess” conductivity in the $x < x_c$ regime is attributed, as mentioned above, to intergrain tunneling^{2,4,5,26} and it is that regime which is of interest here.

Turning to our C-AFM measurements, we show in the insets of Fig. 2(a) typical current images for a sample of 35 vol % Ni for two values of I_{co} , 0.05 and 0.5 nA, in the upper and lower insets, respectively. It is clearly seen that A_t increases with the decrease of I_{co} . For finding the fractal dimension of the three-dimensional percolation cluster D_3 , we recall²² that $D_3 = D + 1$, where D is the fractal dimension of

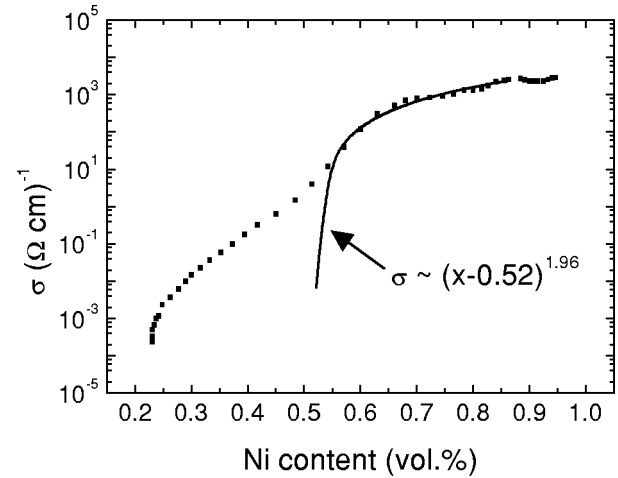


FIG. 1. The dependence of the conductivity of our Ni-SiO₂ composites on the metallic content (in vol % of Ni). The curve represents a fit of the data above the geometrical percolation threshold x_c to Eq. (1).

A_t . The determination of D is carried out by measuring A_t as a function of the “window length” L . In this procedure, we considered L values that are much larger than the particle size but much smaller than the correlation length expected for a percolation network in the vicinity of x_c (tens of microns). For the latter regime, one expects the scaling behavior⁷ $A_t \propto L^D$ with $D = 1.5$ ($D_3 = 2.5$). On the other hand, as one departs from the percolation threshold, D_3 should approach the homogeneous, Euclidian dimension of space, i.e., 3. The two-dimensional images should yield accordingly a value of $D = 1.5$ in the former (x just above x_c) regime and a value of $D = 2$ in the latter ($x \gg x_c$) regime. Indeed, we have previously found this behavior for the CBPC system.²² The corresponding results of our present study on Ni-SiO₂ samples are shown in Fig. 2. The behavior in Fig. 2(a) for $x < x_c$ reveals conductance associated with the network of tunneling transport in the sample. The new observation, in comparison with the findings on CBPC, is that the fractal dimension D decreases with the increase of the I_{co} value considered in the analysis. This effect is beyond the experimental error or the statistical error (of the log-log fit) that is indicated in the figure. The important consequence is that the type of the current network that participates for each I_{co} value is *different* and that for the high I_{co} values, only inter-grain tunneling resistors that are lower than a given value are included in the observed conducting network. The high I_{co} images thus correspond statistically to the contribution of the lowest resistors of the network, i.e., to currents that transverse the sample via a route that consists mainly of particles that are separated by the typical tunneling distance (here, “nearest neighbors”). In contrast, the low I_{co} values include current paths that are added to the above interadjacent grain paths. These additional paths correspond to larger (tunneling) resistors that are either removed nearest neighbors or originate from higher-order neighbors. Hence, the network defined by the highest I_{co} values is similar to the one encountered in fused-particles^{1,5} (or porous media-like) composites,^{8,27} namely, a bona fide percolationlike network.

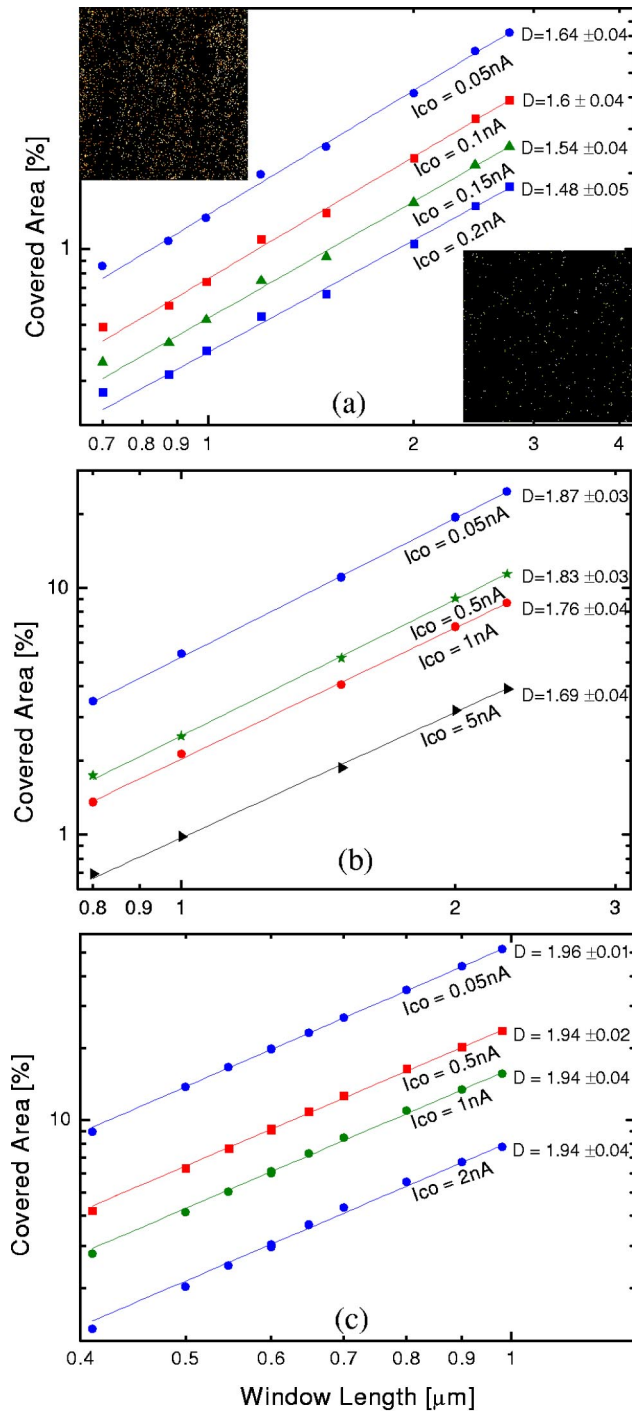


FIG. 2. (Color online) The dependence of the fractional area covered by the “conducting islands” on the “window’s length,” for a few values of the current cutoff: (a) for a sample of $x=35$ Ni vol %, and an applied tip bias of $V=2$ V, (b) $x=60$ vol %, $V=1.6$ V, (c) $x=92$ vol %, $V=1.5$ V. The insets show $5 \times 5 \mu\text{m}^2$ current images measured on the $x=35$ vol % sample, for two values of the current cutoff, 0.05 nA (upper inset) and 0.5 nA (lower inset). The maximum current in both images is 5 nA.

In contrast, the very low I_{co} values correspond to an ACTN that is homogeneous and thus the fractal dimension of the current paths network approaches the regular dimension of the system ($D=2$, $D_3=3$).

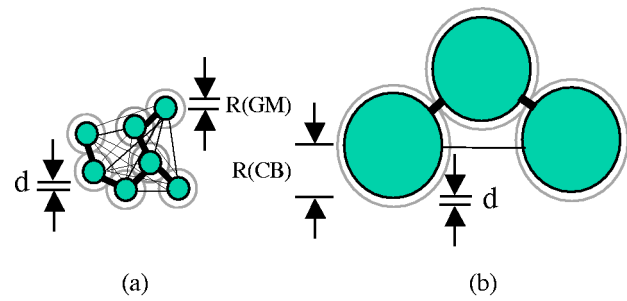


FIG. 3. (Color online) An illustration of small parts of an ACTN. The gray (green) circles represent the conducting particles and their white shells represent the effective tunneling range d . The thick segments represent the tunneling connections between nearest neighbors, while the thin segments represent tunneling connections between higher-order neighbors. The relation between the size of the particles and the tunneling range is illustrated for granular metals in (a) and for carbon black-polymer composites in (b).

The above picture is further supported by the results that are shown in Fig. 2(b) for x just above x_c . Here, we expect *a priori* the fractal dimension of the connected continuous metallic network, i.e., $D_3=2.5$. We note, however, that if we also include now the tunneling contribution in this regime, as was previously suggested by other authors,²⁶ a homogenous tunneling component will be added to the percolation system of the continuous metallic network. Hence, the value of D_3 should increase towards $D_3=3$ with the decrease of I_{co} , as observed. The whole framework of our explanations is validated by the results shown in Fig. 2(c). Here, we see that far above the percolation threshold ($x=92$ vol %) where a genuine homogeneous-continuous network exists, the observed dimension is essentially 3, independent of the value of I_{co} . For comparison, let us mention that for the CBPC the value of D_3 was found to change from 2.5, in the vicinity of x_c , to 3, for $x > x_c$, but *no dependence* on I_{co} has been observed.²²

Another, independent, observation that supports that the above interpretation is derived from the bias dependence of the fractal dimension, which is found to increase monotonically with the tip’s bias. For example, for $x=35$ vol % and $I_{co}=0.05$ nA, the value of D_3 was found to increase from 1.54 at 2V to 1.73 at 3.1 V. Indeed, further conducting channels, involving tunneling between particles with larger interparticle distances, are expected to open up with the increase of bias.²⁶ These channels add to the conduction paths in the ACTN, resulting in a more homogenous network, and consequently a higher value of D (and of D_3).

Our interpretation of the above results now explains well why the percolation predicted⁷ fractal dimension has been observed²² for the CBPC *regardless* of the value of I_{co} . In contrast with the small effective radius of the conducting particles (and then the relatively small distances to particles beyond the nearest neighbor^{2,5}) in the present granular metal systems, $R(GM)$, the effective radius of the carbon particles, $R(CB)$ (~ 100 nm), is very large in comparison with the typical tunneling distance d (a few nanometers).^{3,6,17} Hence, the interparticle surface-to-surface distance of the next nearest neighbors is so much longer in comparison with the corresponding distance of the first nearest neighbors (which is

of the order^{13,17} of d) that the conduction between a given particle and a non-nearest-neighbor is negligible (even in comparison with the conduction in the “insulating” polymer matrix). This picture then explains our finding of *only* $D_3 = 2.5$, as well as the “pure” percolationlike behavior [as manifested by agreement with Eq. (1)] that was generally observed for the CBPC.^{12,13} The fact that a “geometrical” percolationlike correlation length was found¹⁴ in CBPC is also well-explained now. This is since the correlation length was determined by an electrical, rather than a structural, measurement, and thus, as explained above, the corresponding electrical system is a percolation clusterlike system. We see then that for all practical purposes, the CBPC conduct only via nearest-neighbor tunneling. The CBPC constitute then, as do the porous materials,^{20,27} bona fide percolation systems. The above interpretation is illustrated in Fig. 3 where we show two small ACTN systems in which the interparticle tunneling connections are indicated by connecting segments. The thick segments correspond to nearest-neighbor tunneling connections and the thin segments to higher-neighbor tunneling connections. In Fig. 3(a) we illus-

trate the network in the granular metals and in Fig. 3(b) the network in the CBPC. In the former case the thick segments represent the effective network only for high I_{co} values, while in the latter case these are practically the only ones that are effective, for any value of I_{co} . The above interpretation also explains the meaning of x_c in all composite systems where the transport is carried by interparticle tunneling. The experimentally determined value of x_c is the percolation threshold of an electrical network in which *only* the tunneling between adjacent particles contributes to the conduction.

Following all the above, we can conclude that our C-AFM measurements discriminate between various conducting networks. In particular, when the contribution to the conduction is only due to nearest-neighbor tunneling, the system behaves as a genuine percolation system. This explains the pure percolation behavior that is observed in many composites where the conducting particles are geometrically separated from each other and where these are much larger than the tunneling range.

This work was supported in part by the Israel Science Foundation.

*Corresponding author. Electronic address: milode@vms.huji.ac.il

¹B. Abeles, H.L. Pinch, and J.I. Gittleman, Phys. Rev. Lett. **35**, 247 (1975).

²P. Sheng, B. Abeles, and Y. Arie, Phys. Rev. Lett. **31**, 44 (1973).

³P. Sheng, E.K. Sichel, and J.I. Gittleman, Phys. Rev. Lett. **40**, 1197 (1978); and E.K. Sichel, J.I. Gittleman, and P. Sheng, Phys. Rev. B **18**, 5712 (1978).

⁴For a review see B. Abeles *et al.*, Adv. Phys. **24**, 407 (1975).

⁵For a review see, B. Abeles Appl. Solid State Sci. **6**, 1 (1976).

⁶For reviews see, E.K. Sichel, J.I. Gittleman, and P. Sheng, J. Electron. Mater. **11**, 699 (1982); E.K. Sichel, J.I. Gittleman, P. Sheng, in *Carbon Black-Polymer Composites*, edited by E.K. Sichel (Marcel Dekker, New York, 1982).

⁷D. Stauffer and A. Aharony, *Introduction to Percolation Theory* (Taylor and Francis, London, 1992).

⁸I. Balberg and N. Binenbaum, Phys. Rev. B **35**, 8749 (1987).

⁹For a collection of papers, see *Physical Phenomena in Granular Materials*, edited by G.D. Cody, T.H. Geballe, and P. Sheng, Mater. Res. Soc. Symp. Proc. No. 195 (Material Research Society, Pittsburgh, 1990).

¹⁰See, for example, S.T. Chui, Phys. Rev. B **43**, R14276 (1991); P. Sheng, Philos. Mag. B **65**, 357 (1992); M. Pollak and C. J. Adkins, *ibid.* **65**, 855 (1992).

¹¹J.H. Smuckler and P. Finnerty, Adv. Chem. Ser. **134**, 171 (1974).

¹²See for example, I. Balberg and S. Bozowski, Solid State Commun. **44**, 551 (1982); M.B. Heaney, Phys. Rev. B **52**, 12 477

(1995); P. Mandal *et al.*, *ibid.* **55**, 452 (1997); D. van der Putten *et al.*, Phys. Rev. Lett. **69**, 494 (1992).

¹³S.H. Foulger, J. Appl. Polym. Sci. **72**, 1573 (1999).

¹⁴I. Balberg and J. Blanc, Phys. Rev. B **31**, 8295 (1985).

¹⁵See, for example, C.C. Chen and Y.C. Chou, Phys. Rev. Lett. **54**, 2529 (1985); A. Celzand *et al.*, Phys. Rev. B **53**, 6209 (1996); L. Flandin *et al.*, J. Appl. Polym. Sci. **76**, 894 (2000).

¹⁶For a review of data on many composites, see J. Wu and D.S. Mclachlan, Phys. Rev. B **56**, 1236 (1997).

¹⁷I. Balberg, Phys. Rev. Lett. **53**, 1305 (1987); Z. Rubin *et al.*, Phys. Rev. B **59**, 12 196 (1999).

¹⁸For a recent example, see M.T. Connor *et al.*, Phys. Rev. B **57**, 2286 (1998).

¹⁹I. Balberg, Carbon **40**, 139 (2002).

²⁰For a review, see M.B. Isichenko, Rev. Mod. Phys. **64**, 961 (1992).

²¹E.Z. Luo *et al.*, Phys. Rev. B **57**, R15120 (1998), and references therein.

²²N. Shimoni *et al.*, Phys. Rev. B **66**, 020102R (2002).

²³S. Barzilai *et al.*, Phys. Rev. B **23**, 1809 (1981).

²⁴M. Rayl *et al.*, Phys. Lett. **36A**, 477 (1971).

²⁵J.I. Gittleman, Y. Goldstein, and S. Bozowski, Phys. Rev. B **5**, 3609 (1972).

²⁶J.V. Mantese, W.A. Curtin, and W.W. Web, Phys. Rev. B **33**, 7897 (1986).

²⁷For a review, see I. Balberg, Phys. Rev. B **57**, 13 351 (1998).